Supporting Information

pH/ROS Dual-Responsive Supramolecular Vesicles Fabricated by Carboxylated Pillar[6]arene-Based Host-Guest Recognition and Phenylboronic Acid Pinacol Ester Derivative

Qi Hao, Yuetong Kang, Jiang-Fei Xu, and Xi Zhang*

Key Lab of Optoelectronics & Molecular Engineering, Department of Chemistry, Tsinghua University, Beijing 100084, China

E-mail: xujf@mail.tsinghua.edu.cn

Number of pages: 30

Number of figures: 37

Number of schemes: 2

Number of tables: 1

Table of Contents

1. Synthesis and characterization of PBEC$_n$A and C$_{12}$AH

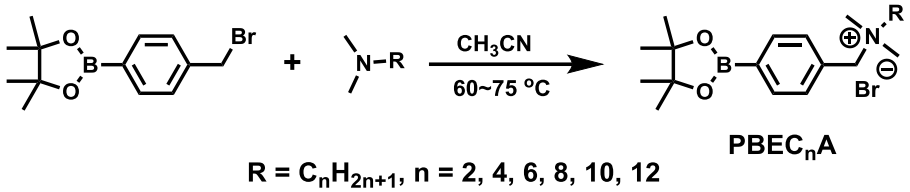

Scheme S1. Synthesis of PBEC$_n$A

Synthesis of PBEC$_2$A

The synthesis procedure of PBEC$_2$A is conducted as follows. 4-(Bromomethyl)phenylboronic acid pinacol ester (0.51 g, 1.72 mmol) and N,N-dimethylethylamine (0.11 g, 1.50 mmol) were dissolved in 10 mL of acetonitrile, and the mixture was stirred and heated at 60 °C for 8 h. Next, the mixture was concentrated by rotary evaporator to half volume. Then, the solution was dropwise added to 150 mL of diethyl ether. The formed precipitate was filtered and washed with diethyl ether, then dried in vacuum to obtain the white solid, yielding 77%.

^{1}H NMR (D_2O, 600 MHz): δ 7.86 (d, J = 7.8 Hz, 2H), 7.55 (d, J = 7.8 Hz, 2H), 4.48 (s, 2H), 3.39 (q, J = 7.2 Hz, 2H), 2.98 (s, 6H), 1.42 (t, J = 7.2 Hz, 3H), 1.20 (s, 12H).

^{13}C NMR (D_2O, 150 MHz): δ 134.23, 132.35, 129.56, 75.74, 67.21, 60.07, 49.14, 23.85, 7.72.

MS (ESI): found m/z = 290.228, calculated m/z for ([M – Br] $^+$) = 290.229.

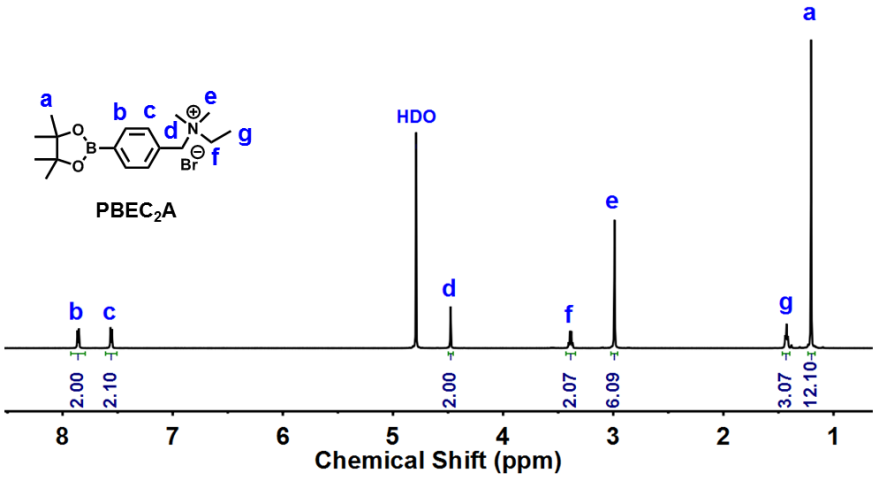

Figure S1. ^{1}H NMR spectrum (D_2O, 600 MHz) of PBEC$_2$A.

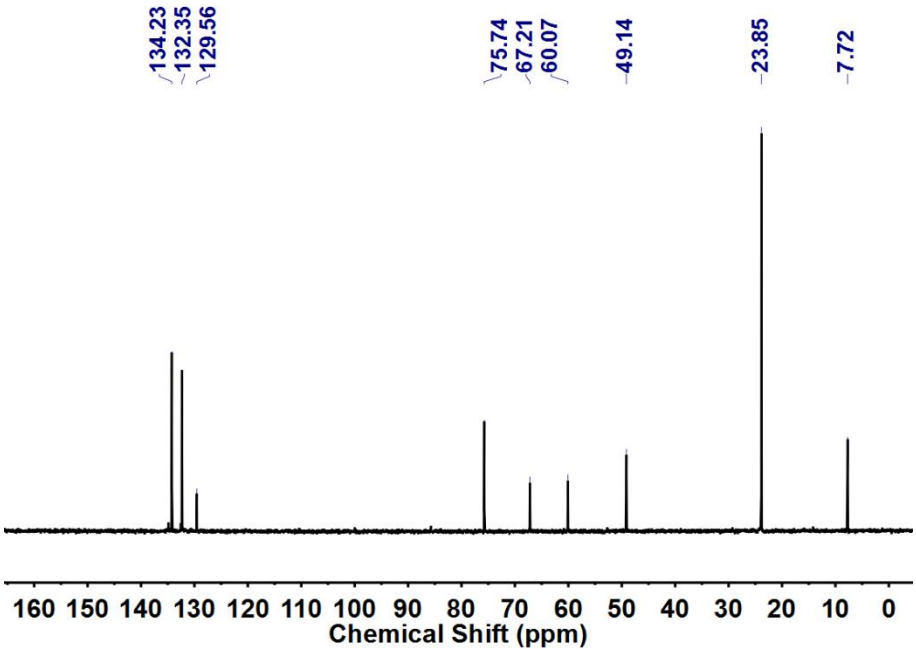

Figure S2. ^{13}C NMR spectrum (D_2O, 150 MHz) of $PBEC_2A$.

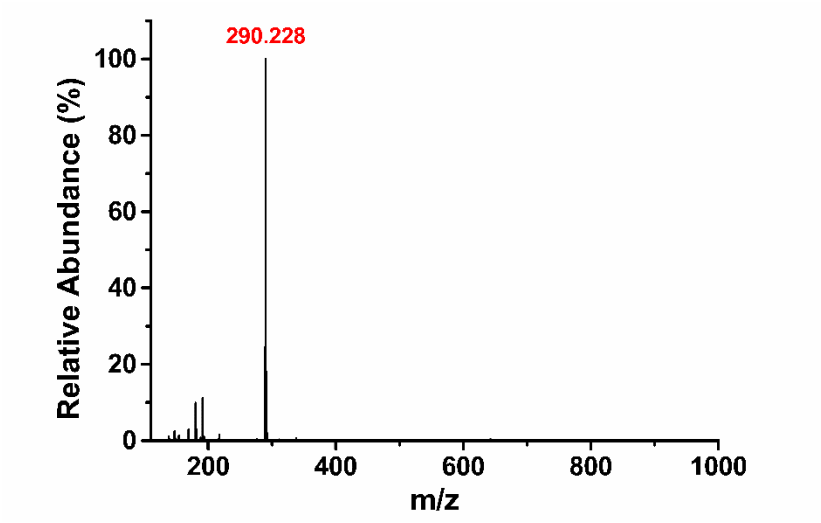

Figure S3. MS(ESI) of $PBEC_2A$.

Synthesis of PBEC$_4$A

4-(Bromomethyl)phenylboronic acid pinacol ester (0.45 g, 1.52 mmol) and N,N-dimethylbutylamine (0.12 g, 1.18 mmol) were dissolved in 10 mL of acetonitrile, and the mixture was stirred and heated at 65 ^{o}C for 8 h. After evaporation, the residue was re-dissolved in 5 mL of methanol. Then, the mixture was precipitated in 150 mL of diethyl ether and filtrated then dried in vacuum to give white product yielding 91%.

^{1}H NMR (DMSO-d_6, 600 MHz): δ 7.78 (d, J = 7.8 Hz, 2H), 7.55 (d, J = 7.8 Hz, 2H), 4.53 (s, 2H), 3.25 (m, 2H), 2.94 (s, 6H), 1.77 (m, 2H), 1.30 (m, 14H), 0.95 (t, J = 7.2 Hz, 3H).

^{13}C NMR (DMSO-d_6, 150 MHz): δ 134.70, 132.39, 131.10, 83.96, 65.95, 63.35, 49.19, 24.64, 23.75, 19.24, 13.50.

MS (ESI): found m/z = 318.259, calculated m/z for ([M – Br] $^{+}$) = 318.260.

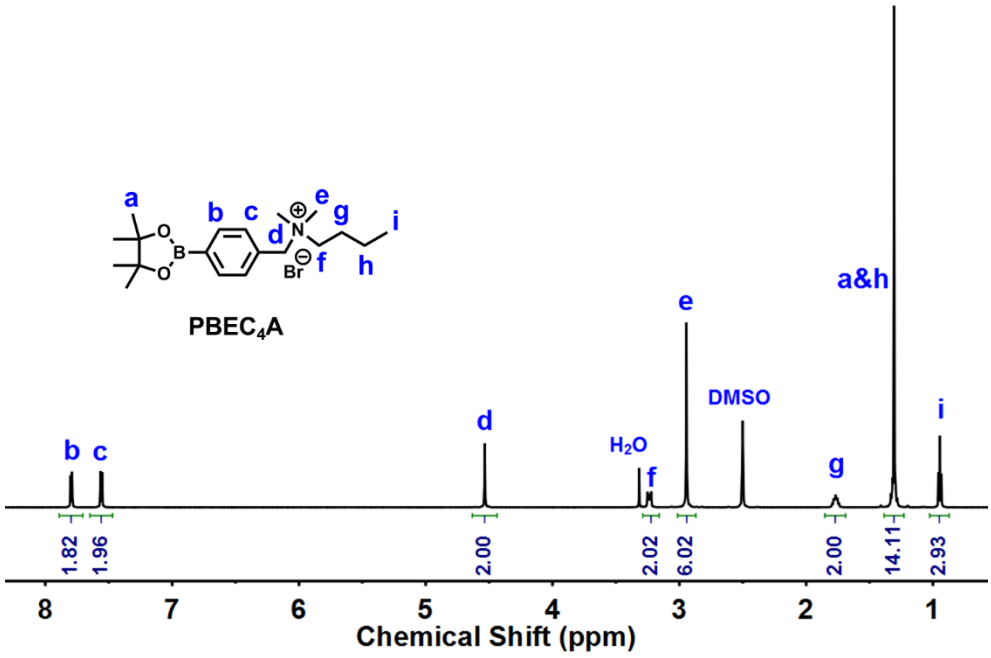

Figure S4. ^{1}H NMR spectrum (DMSO-d_6, 600 MHz) of PBEC$_4$A.

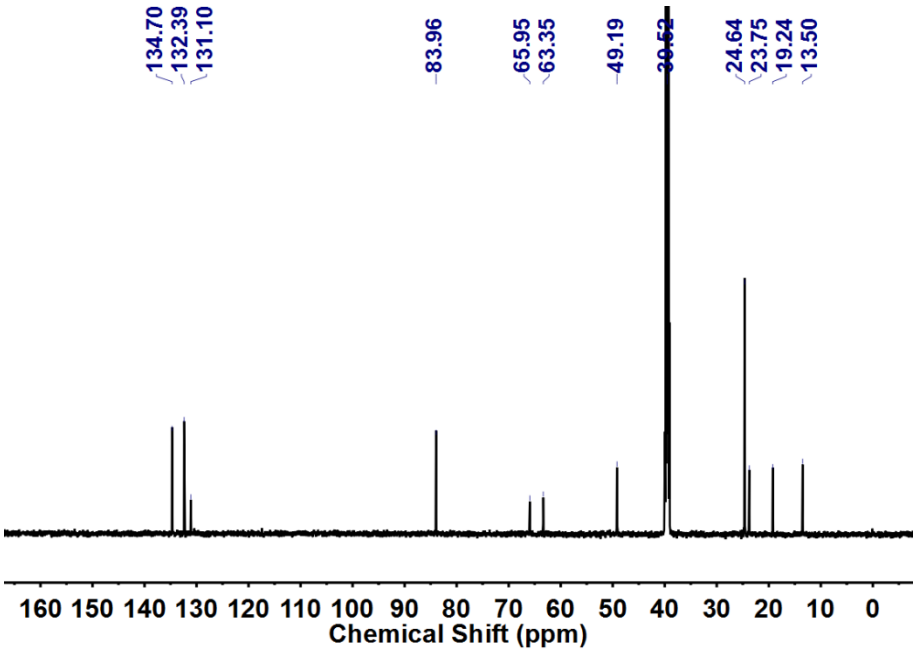

Figure S5. ^{13}C NMR spectrum (DMSO-d_6, 150 MHz) of PBEC$_4$A.

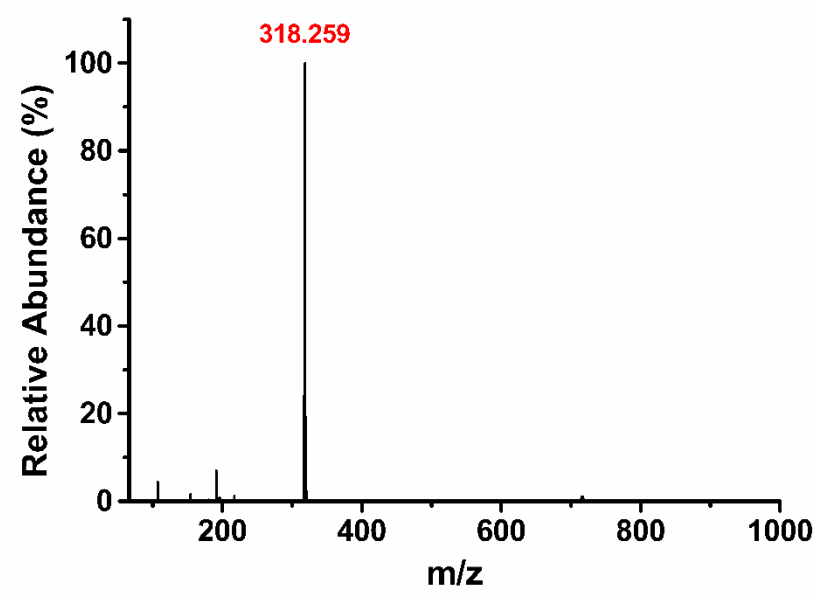

Figure S6. MS(ESI) of PBEC$_4$ A.

Synthesis of PBEC$_6$N

4-(Bromomethyl)phenylboronic acid pinacol ester (0.67 g, 2.26 mmol) and N,N-dimethylhexylamine (0.26 g, 2.01 mmol) were dissolved in 10 mL of acetonitrile, and the mixture was stirred and heated at 60 ^{o}C overnight. Next, the mixture was concentrated by rotary evaporator to half volume. Then, the mixture was precipitated in 150 mL of diethyl ether and filtrated then dried in vacuum to give white product yielding 90%.

^{1}H NMR (600 MHz, DMSO-d_6): δ 7.78 (d, J = 8.4 Hz, 2H), 7.55 (d, J = 8.4 Hz, 2H), 4.55 (s, 2H), 3.25 (m, 2H), 2.94 (s, 6H), 1.77 (m, 2H), 1.30 (m, 18H), 0.88 (t, J = 7.2 Hz, 3H)

^{13}C NMR (150 MHz, DMSO-d_6): δ 134.70, 132.38, 131.11, 83.96, 65.95, 63.55, 49.16, 30.65, 25.44, 24.64, 21.82, 13.80.

MS (ESI): found m/z = 346.290, calculated m/z for ([M – Br] $^{+}$) = 346.291.

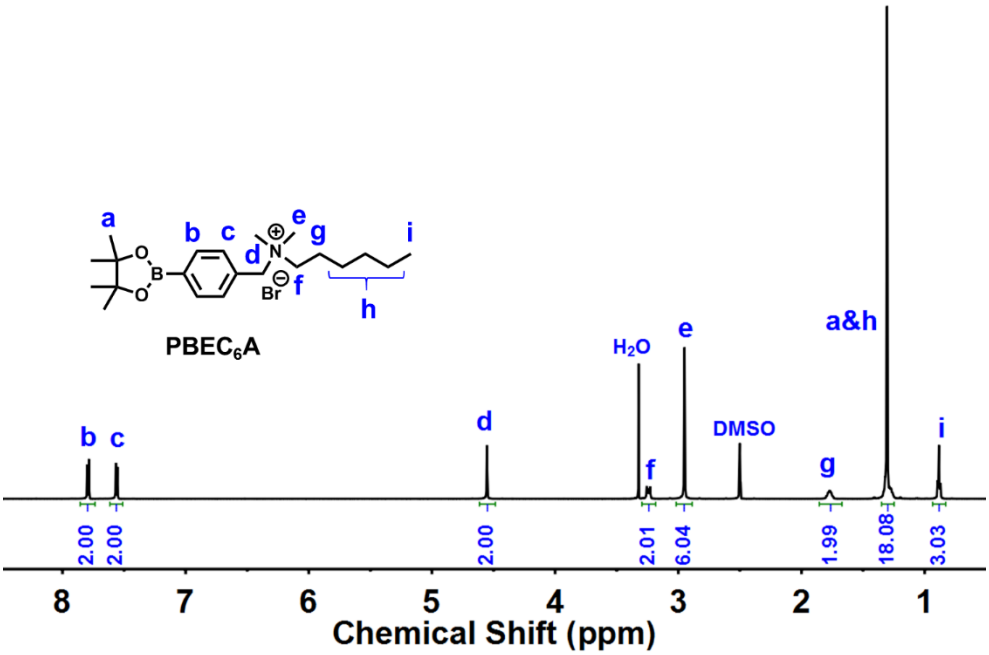

Figure S7. ^{1}H NMR spectrum (DMSO-d_6, 600 MHz) of PBEC$_6$A.

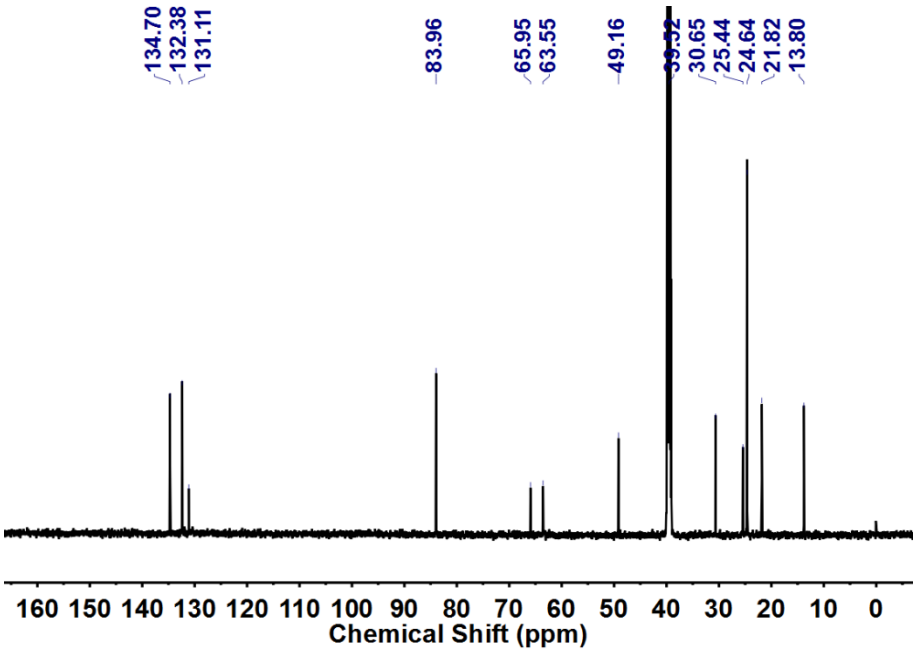

Figure S8. ^{13}C NMR spectrum (DMSO-d_6, 150 MHz) of PBEC$_6$A.

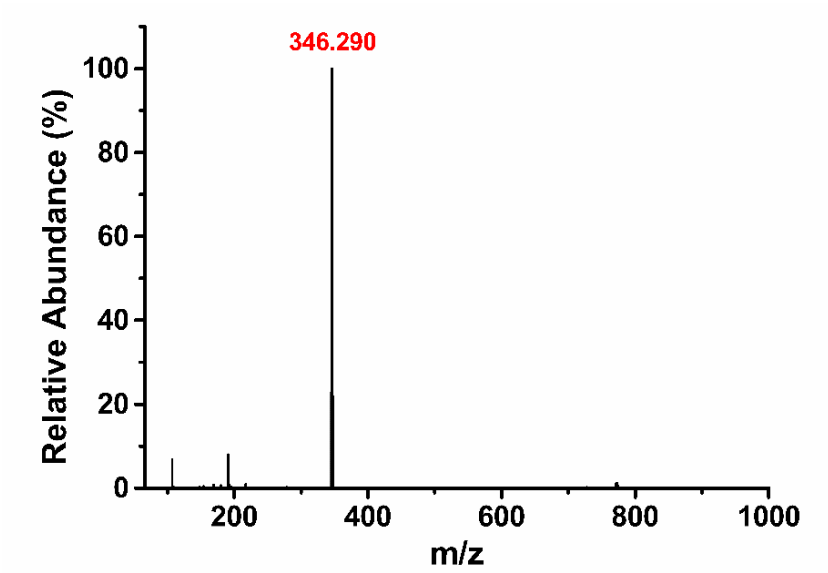

Figure S9. MS(ESI) of PBEC$_6$ A.

Synthesis of PBEC$_8$A.

4-(Bromomethyl)phenylboronic acid pinacol ester (0.88 g, 2.96 mmol) and N,N-dimethyloctylamine (0.34 g, 2.16 mmol) were dissolved in 15 mL of acetonitrile, and the mixture was stirred and heated at 70 ^{o}C for 8 h. Next, the mixture was concentrated by rotary evaporator and the residue was re-dissolved in 5 mL of chloroform. Then, the mixture was precipitated in 150 mL of petroleum ether and filtrated then dried in vacuum, faint yellow solid product was obtained with a yield of 59%.

^{1}H NMR (600 MHz, DMSO-d_6): δ 7.78 (d, J = 7.8 Hz, 2H), 7.56 (d, J = 7.8 Hz, 2H), 4.53 (s, 2H), 3.21 (m, 2H), 2.94 (s, 6H), 1.77 (m, 2H), 1.30 (m, 22H), 0.87 (t, J = 6.6 Hz, 3H)

^{13}C NMR (150 MHz, DMSO-d_6): δ 134.70, 132.37, 131.12, 100.10, 83.96, 65.97, 63.54, 49.18, 31.14, 28.41, 25.79, 24.64, 22.03, 13.94.

MS (ESI): found m/z = 374.322, calculated m/z for ([M – Br] $^{+}$) = 374.322.

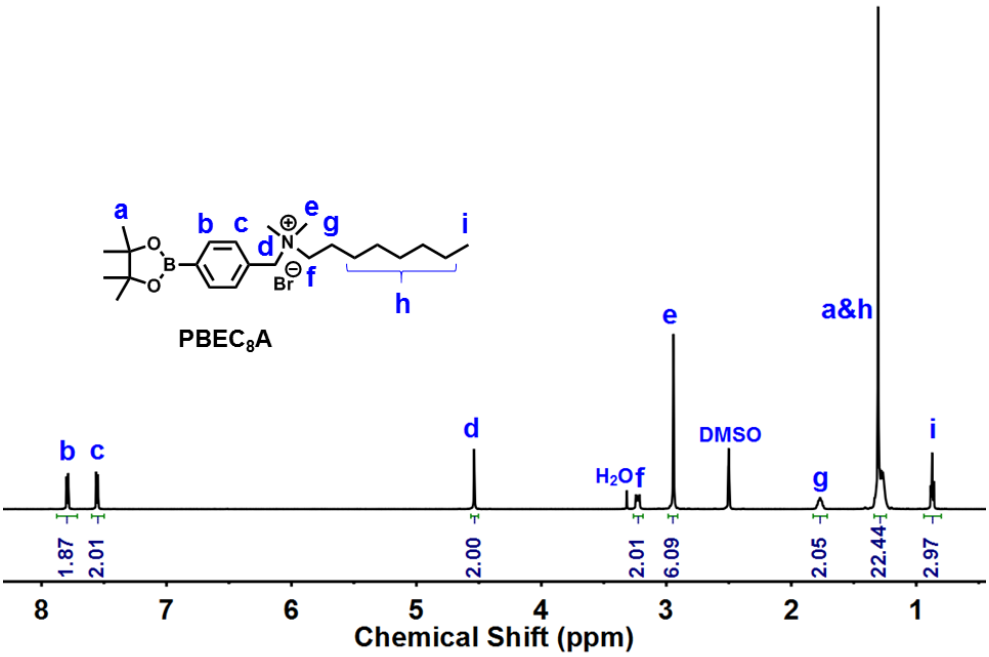

Figure S10. ^{1}H NMR spectrum (DMSO-d_6, 600 MHz) of PBEC$_8$A.

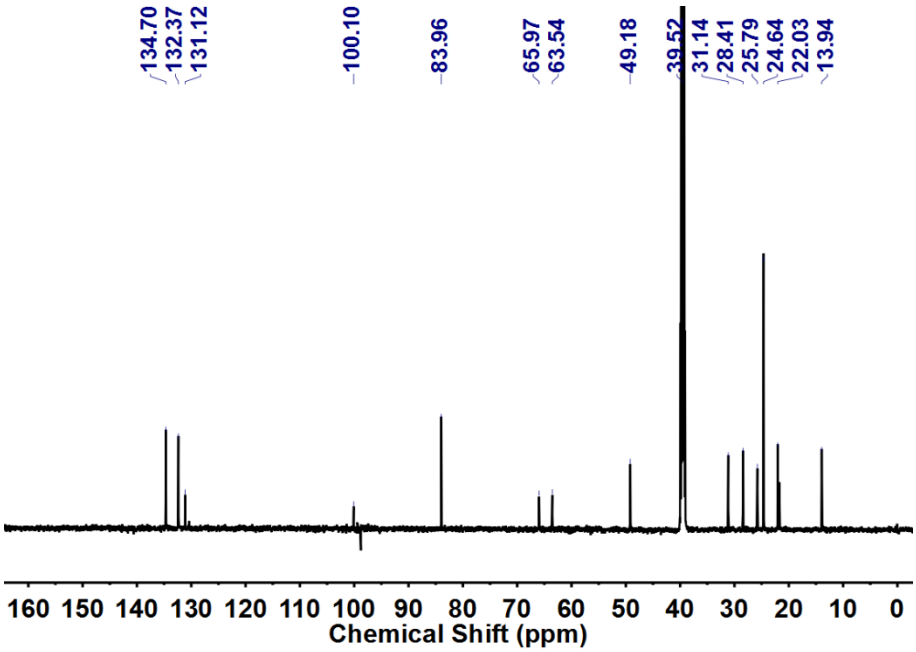

Figure S11. ^{13}C NMR spectrum (DMSO-d_6, 150 MHz) of PBEC$_8$A.

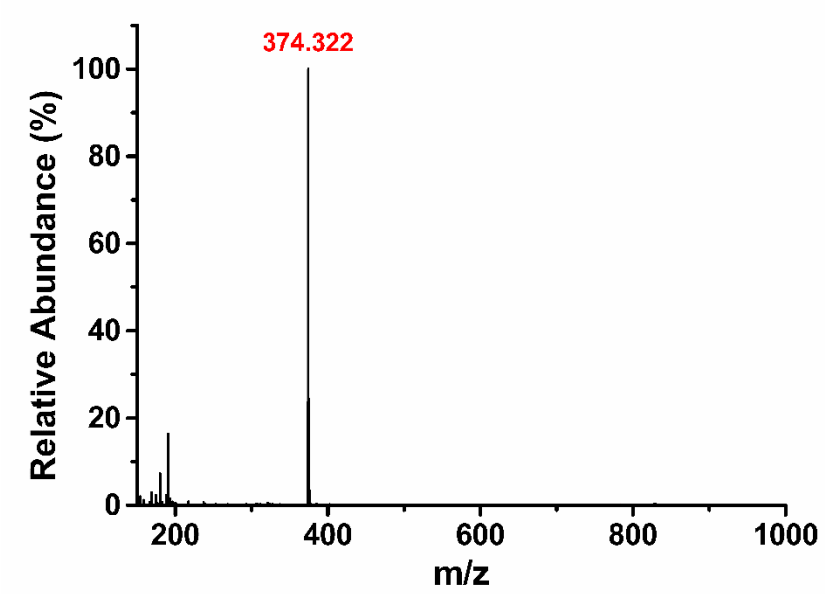

Figure S12. MS(ESI) of PBEC$_8$ A.

Synthesis of PBEC$_{10}$A.

4-(Bromomethyl)phenylboronic acid pinacol ester (0.70 g, 2.36 mmol) and N,N-dimethyldecylamine (0.37 g, 2.00 mmol) were dissolved in 10 mL of acetonitrile, and the mixture was stirred and heated at 70 ^{o}C overnight. Next, the mixture was concentrated by rotary evaporator and the residue was re-dissolved in 5 mL of chloroform. Then, the mixture was precipitated in 150 mL of petroleum ether and then dried in vacuum, faint yellow solid product was obtained with a yield of 55%.

^{1}H NMR (600 MHz, DMSO-d_6): δ 7.78 (d, J = 7.8 Hz, 2H), 7.56 (d, J = 7.8 Hz, 2H), 4.54 (s, 2H), 3.21 (m, 2H), 2.94 (s, 6H), 1.76 (m, 2H), 1.30-1.26 (m, 26H), 0.86 (t, J = 6.6 Hz, 3H)

^{13}C NMR (150 MHz, DMSO-d_6): δ 134.68, 132.37, 131.13, 83.94, 65.90, 63.48, 49.17, 31.26, 28.85, 28.75, 28.63, 28.46, 25.77, 24.63, 22.07, 21.75, 13.93.

MS (ESI): found m/z = 402.354, calculated m/z for ([M – Br] $^{+}$) = 420.354.

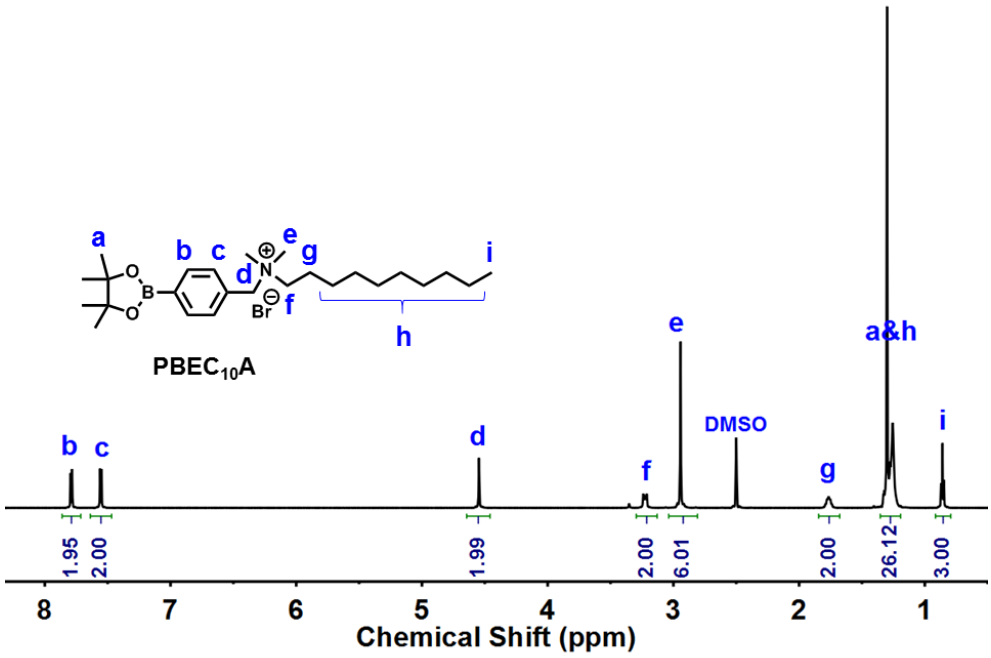

Figure S13. ^{1}H NMR spectrum (DMSO-d_6, 600 MHz) of PBEC$_{10}$A.

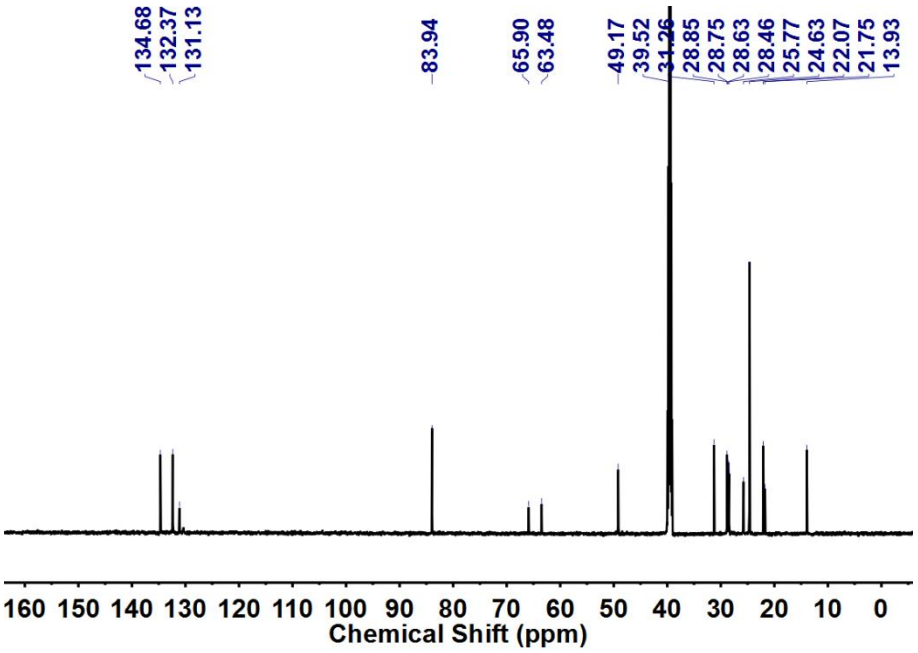

Figure S14. ^{13}C NMR spectrum (DMSO-d_6, 150 MHz) of PBEC$_{10}$A.

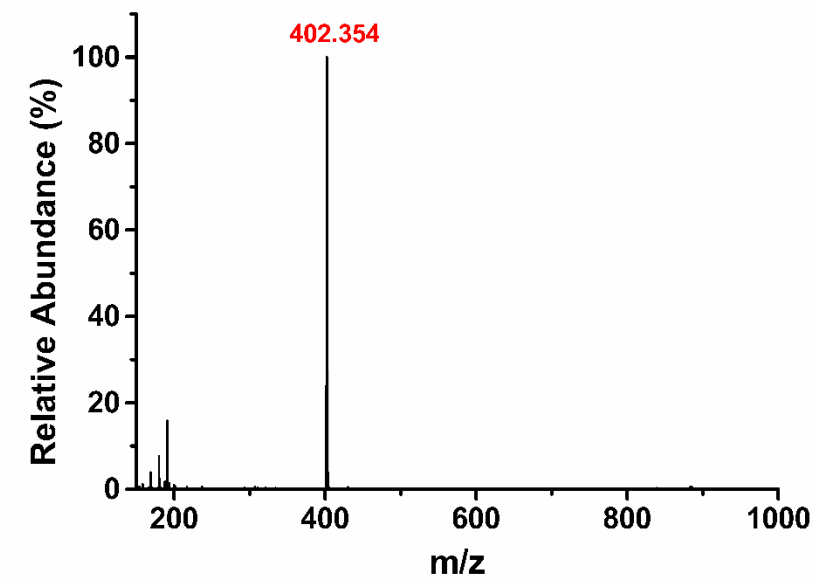

Figure S15. MS(ESI) of PBEC$_{10}$ A.

Synthesis of PBEC$_{12}$A.

4-(Bromomethyl)phenylboronic acid pinacol ester (0.77 g, 2.59 mmol) and N,N-dimethyldodecylamine (0.48 g, 2.25 mmol) were dissolved in 10 mL of acetonitrile, and the mixture was stirred and heated at 75 ^{o}C overnight. After evaporation, the residue was re-dissolved in 5 mL of chloroform. Then, the mixture was precipitated in 150 mL of petroleum ether and filtrated then dried in vacuum, faint yellow solid product was obtained with a yield of 59%.

^{1}H NMR (600 MHz, DMSO-d_6): δ 7.79 (d, J = 8.4 Hz, 2H), 7.56 (d, J = 8.4 Hz, 2H), 4.53 (s, 2H), 3.22 (m, 2H), 2.94 (s, 6H), 1.77 (m, 2H), 1.30 - 1.25 (m, 30H), 0.85 (t, J = 6.6 Hz, 3H)

^{13}C NMR (150 MHz, DMSO-d_6): δ 134.68, 132.36, 131.12, 83.95, 65.91, 63.48, 49.18, 31.27, 28.98, 28.89, 28.74, 28.68, 28.45, 25.77, 24.63, 22.06, 21.75, 13.93.

MS (ESI): found m/z = 430.384, calculated m/z for ([M – Br] $^{+}$) = 430.385.

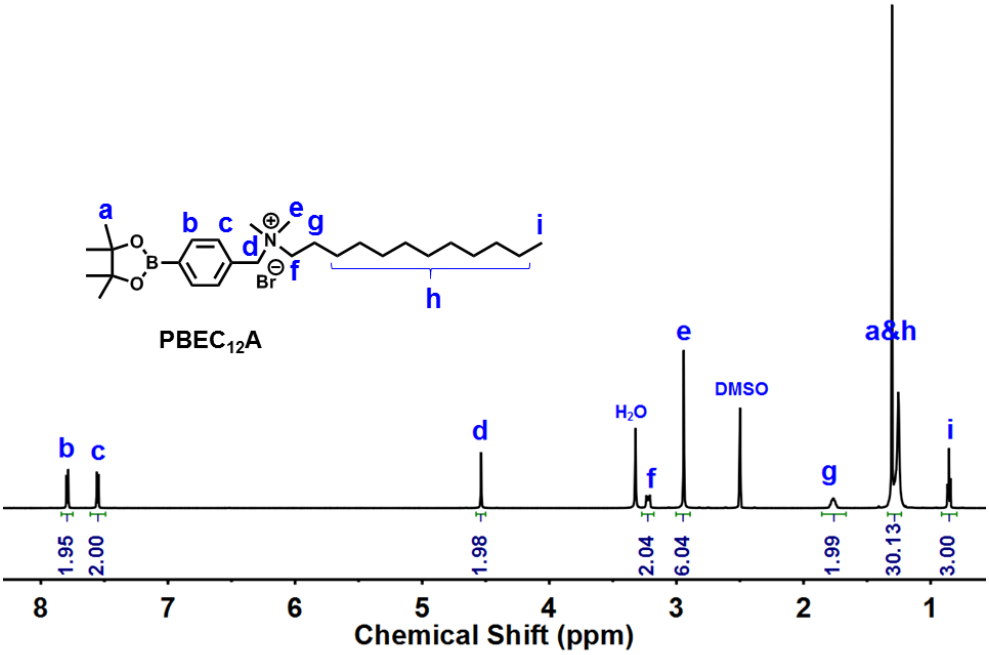

Figure S16. ^{1}H NMR spectrum (DMSO-d_6, 600 MHz) of PBEC$_{12}$A.

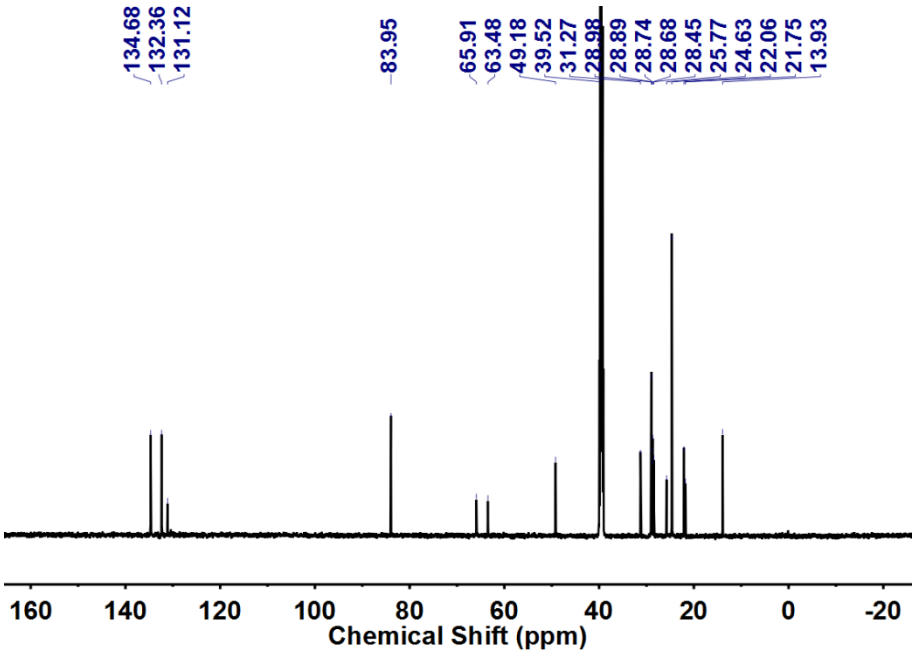

Figure S17. ^{13}C NMR spectrum (DMSO-d_6, 150 MHz) of PBEC$_{12}$A.

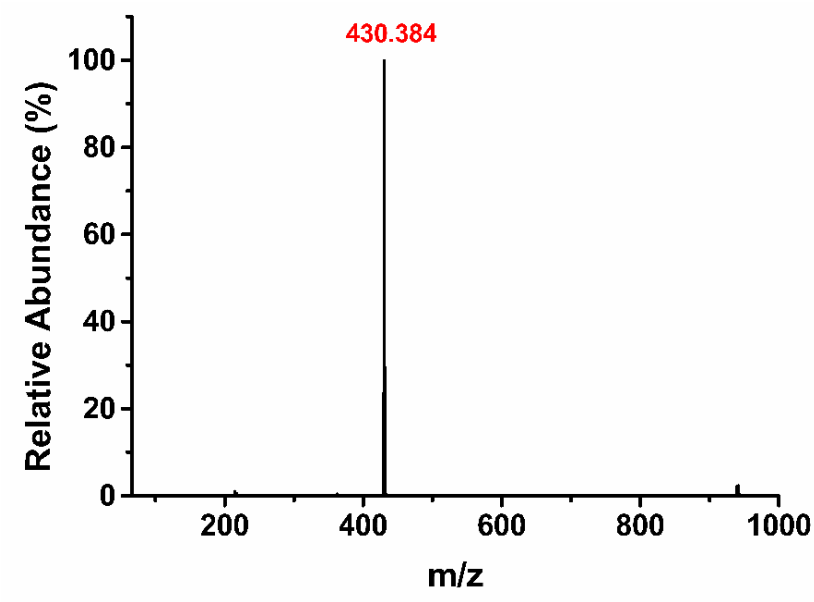

Figure S18. MS(ESI) of PBEC$_{12}$A.

Synthesis of $C_{12}AH$

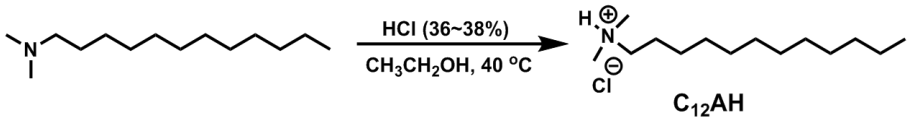

Scheme S2. Synthesis of $C_{12}AH$

N,N-dimethyldodecylamine (1.64 g, 7.68 mmol) were dissolved in 20 mL of ethanol, then the concentrated hydrochloric acid (1.4 mL, 36~38 %) was dropwise added. The mixture was stirred and heated at 40 °C for 5 h. After evaporation, the residue was re-dissolved in 5 mL of chloroform. Then, the mixture was precipitated in 150 mL of petroleum ether and centrifuged then dried in vacuum, white solid product was obtained with a yield of 29%.

^{1}H NMR (600 MHz, $CDCl_3$): δ 12.24 (br, 1H), 2.94 (m, 2H), 2.77 (d, J = 4.8 Hz, 6H), 1.81 (m, 2H), 1.30-1.21 (m, 18H), 0.84 (t, J = 6.6 Hz, 3H).

^{13}C NMR (150 MHz, $CDCl_3$): δ 58.06, 42.83, 31.94, 29.61, 29.51, 29.37, 29.08, 26.71, 24.26, 22.73, 14.18.

MS (ESI): found m/z = 214.253, calculated m/z for ($[M - Br]^+$) = 214.253.

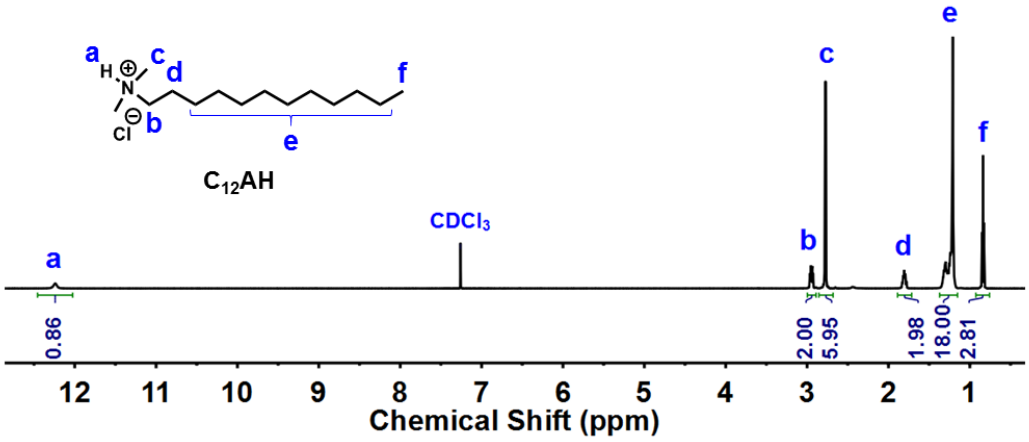

Figure S19. ^{1}H NMR spectrum ($CDCl_3$, 600 MHz) of $C_{12}AH$.

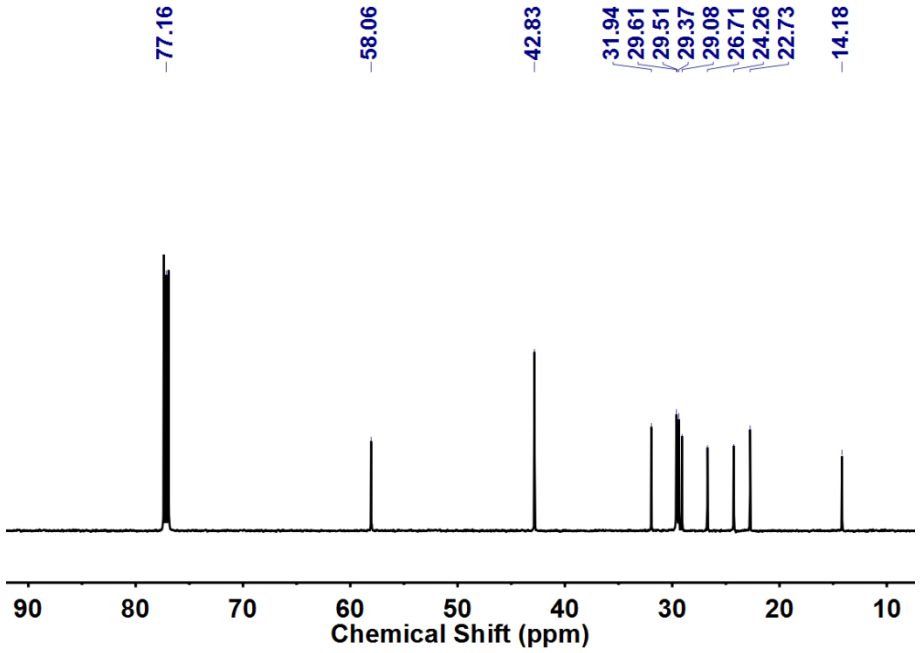

Figure S20. ^{13}C NMR spectrum ($CDCl_3$, 150 MHz) of $C_{12}AH$.

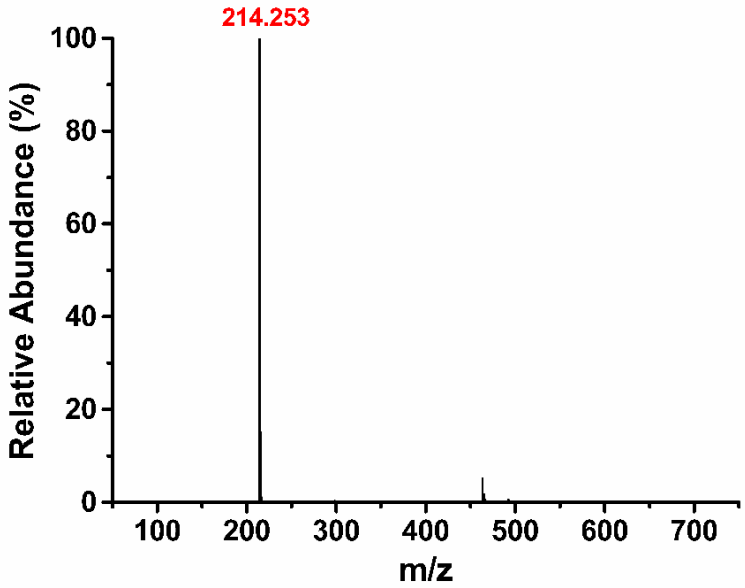

Figure S21. MS(ESI) of $C_{12}AH$.

2. Isothermal titration calorimetry data of PBEC$_n$A (n = 2, 4, 6, 8, 10)

The ITC experiments were performed by titrating the guest molecule into the CP[6] host in 20 mM phosphate buffer of pH 7.4 at 37.0 ^{o}C. The titration curves of 1:1 complexations between all the guests and CP[6] were shown as following:

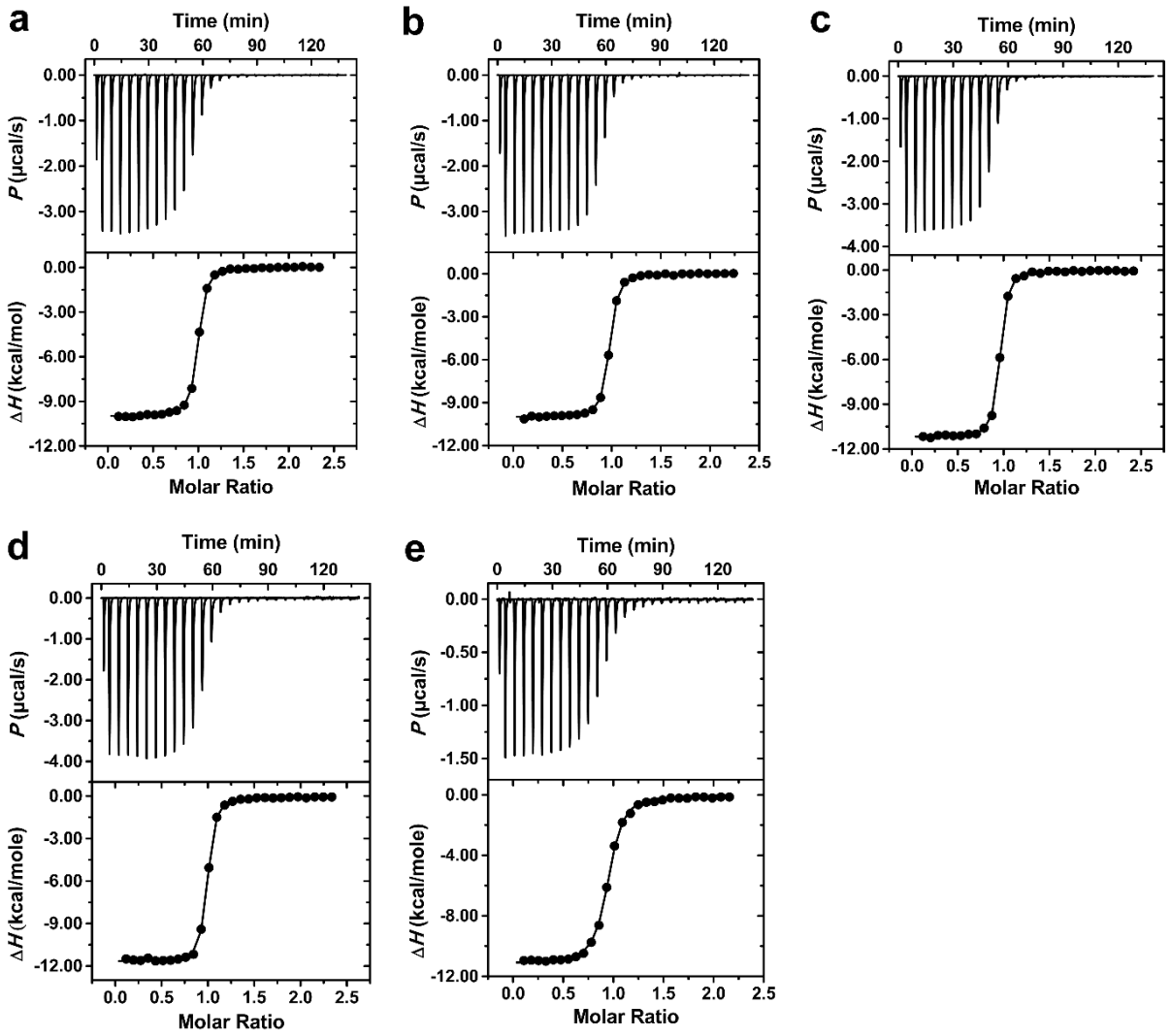

Figure S22. ITC data and fitting curves for the titrations of (a) PBEC$_2$A (1.0 mM) into CP[6] (0.10 mM) (b) PBEC$_4$A (1.0 mM) into CP[6] (0.10 mM) (c) PBEC$_6$A (1.0 mM) into CP[6] (0.10 mM) (d) PBEC$_8$A (1.0 mM) into CP[6] (0.10 mM) (e) PBEC$_{10}$A (0.4 mM) into CP[6] (0.040 mM).

3. Thermodynamic data of the PBEC$_n$A-CP[6] host−guest complexation

Table S1. Binding constants (K_a) and the relevant thermodynamic parameters for the complexation of PBEC$_n$A (n = 2, 4, 6, 8, 10, 12) with the host CP[6]. [a]

Guest	K_a (10^6 M^{-1})	ΔH (kcal/mol)	$T\Delta S$ (kcal/mol)
PBEC$_2$A	6.20 ± 0.22	-9.995 ± 0.015	-0.04
PBEC$_4$A	6.80 ± 0.25	-10.010 ± 0.015	-0.04
PBEC$_6$A	7.10 ± 0.35	-11.190 ± 0.023	-0.18
PBEC$_8$A	6.77 ± 0.46	-11.670 ± 0.034	-0.24
PBEC$_{10}$A	4.59 ± 0.27	-11.160 ± 0.045	-0.20
PBEC$_{12}$A	3.44 ± 0.16	-12.110 ± 0.044	-0.34

[a] In 20 mM phosphate buffer solution at T = 310 K

4. The critical aggregation concentration (CAC) of $PBEC_{12}A$

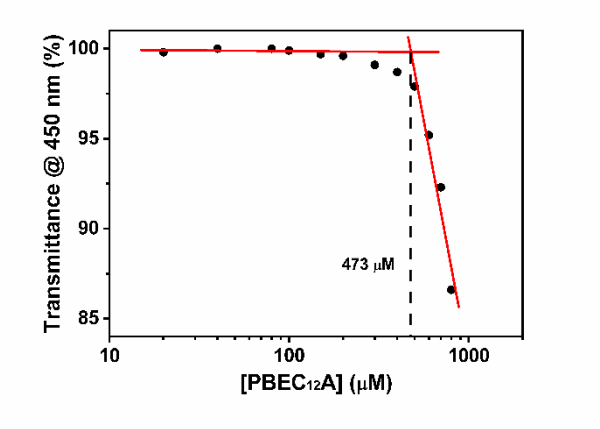

Figure S23. CAC of $PBEC_{12}A$ measured by concentration-dependent optical transmittance method according to the previously published literature. [1]

5. UV-vis spectra of $PBEC_{12}A$ before and after adding CP[6]

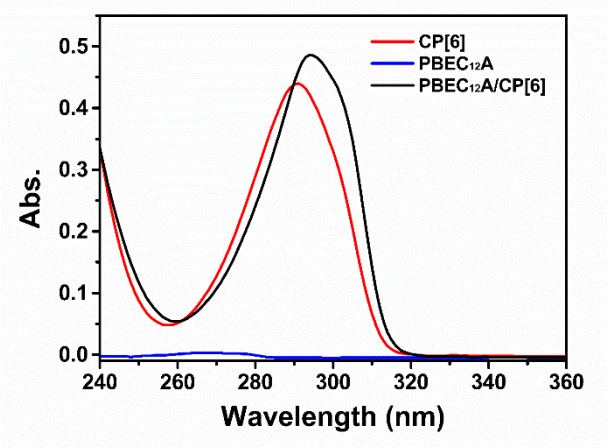

Figure S24. UV/Vis absorption spectra of $PBEC_{12}A$ (100 μM) and $PBEC_{12}A$-CP[6] (100 μM) complex in aqueous solution. (path length was 2.0 mm)

CP[6] displayed a maximum absorption peak at 290 nm, and $PBEC_{12}A$ showed weak absorption in the range of whole spectrum. After addition of 1.0 equiv of $PBEC_{12}A$, the characteristic absorption of CP[6] slightly increased and the maximum wavelength shifted to 294 nm, which may result from the strong host–guest complexation between CP[6] and $PBEC_{12}A$.

6. The CAC of PBEC$_{12}$A-CP[6] (5:1) and PBEC$_{12}$A-CP[6] (10:1)

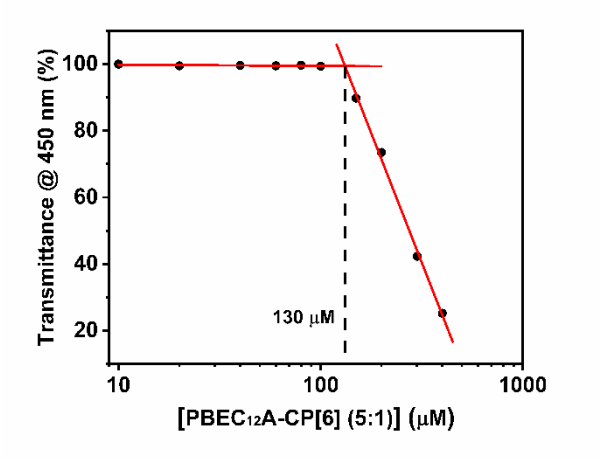

Figure S25. CAC of PBEC$_{12}$A-CP[6] (5:1) measured by concentration-dependent optical transmittance method.

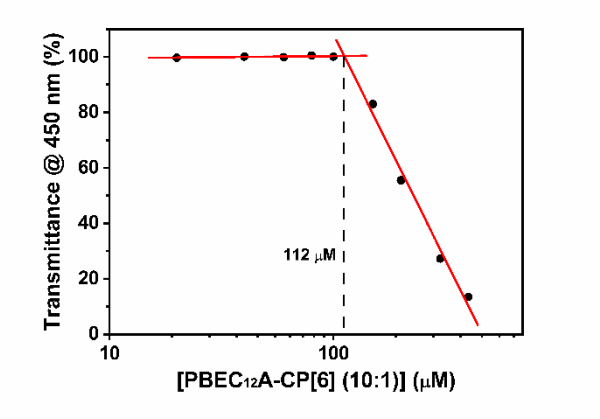

Figure S26. CAC of PBEC$_{12}$A-CP[6] (10:1) measured by concentration-dependent optical transmittance method.

7. The original HRTEM images of self-assemblies from PBEC$_{12}$A-CP[6] supramolecular complex at different host-guest ratios

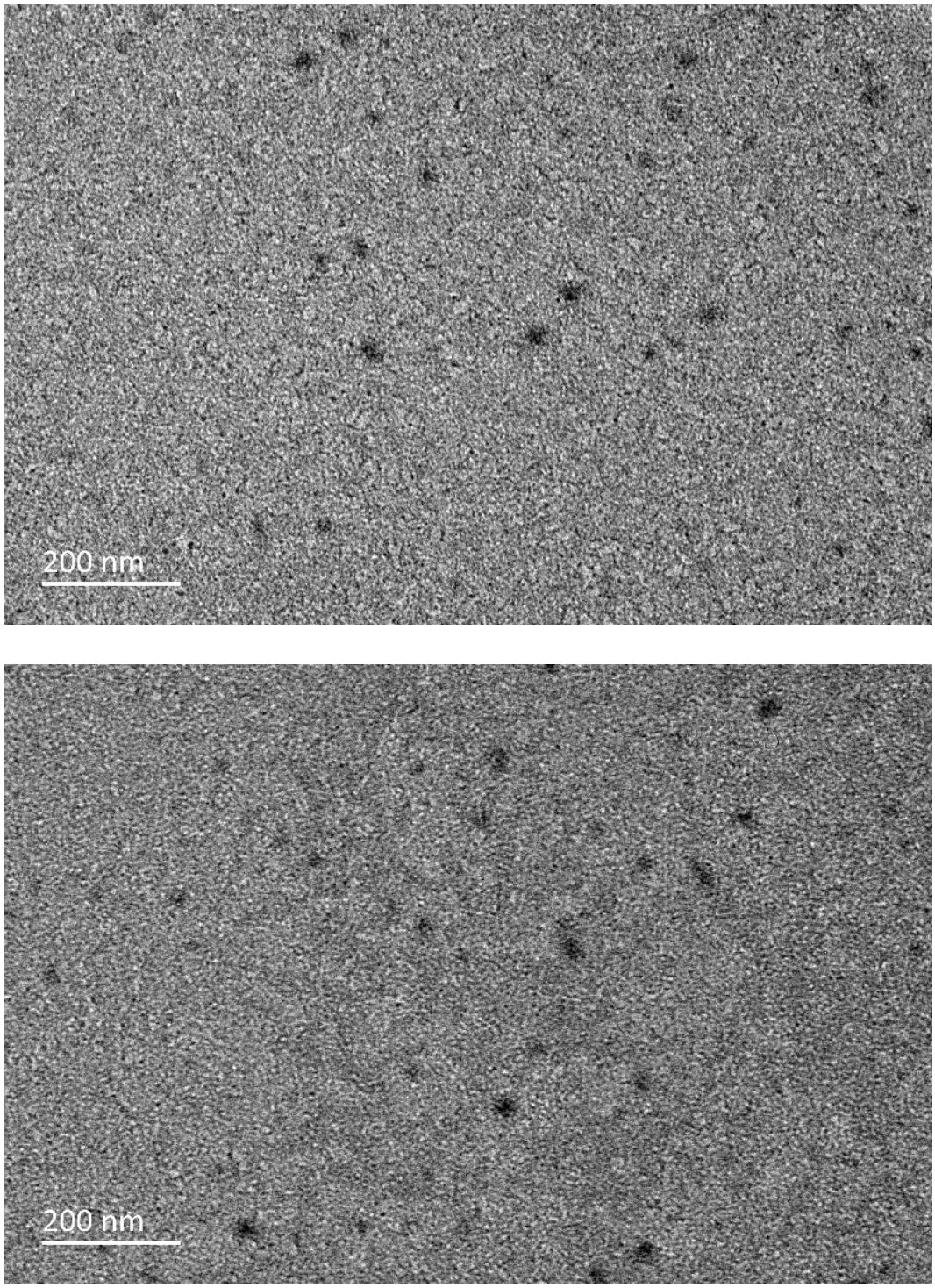

Figure S27. Original HRTEM images showing the self-assembly structures of PBEC$_{12}$A alone.

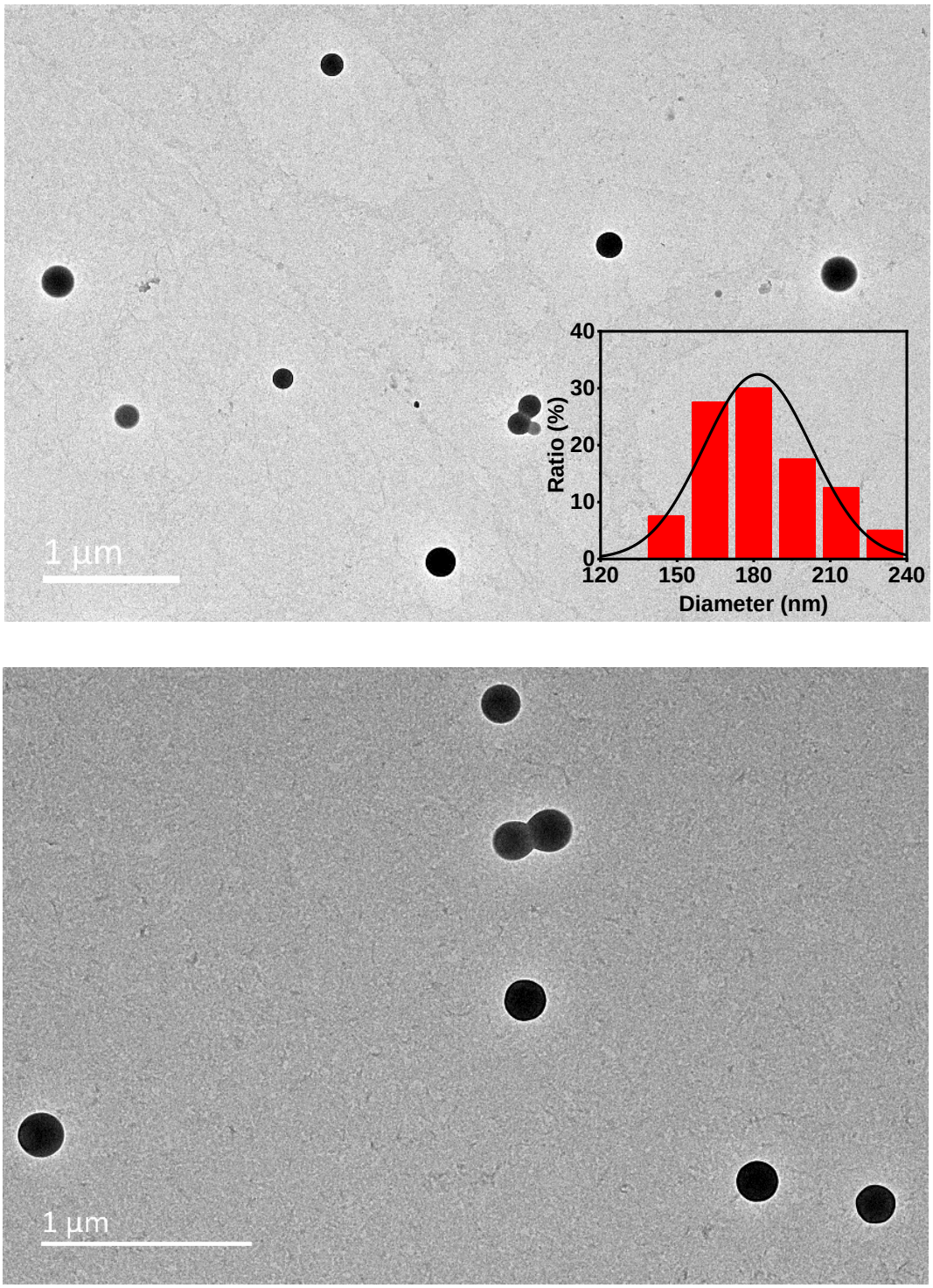

Figure S28. Original HRTEM images showing the self-assembly structures of PBEC$_{12}$A-CP[6] at molar ratio of 20:1. Inset: the histogram analysis of the diameter of vesicles.

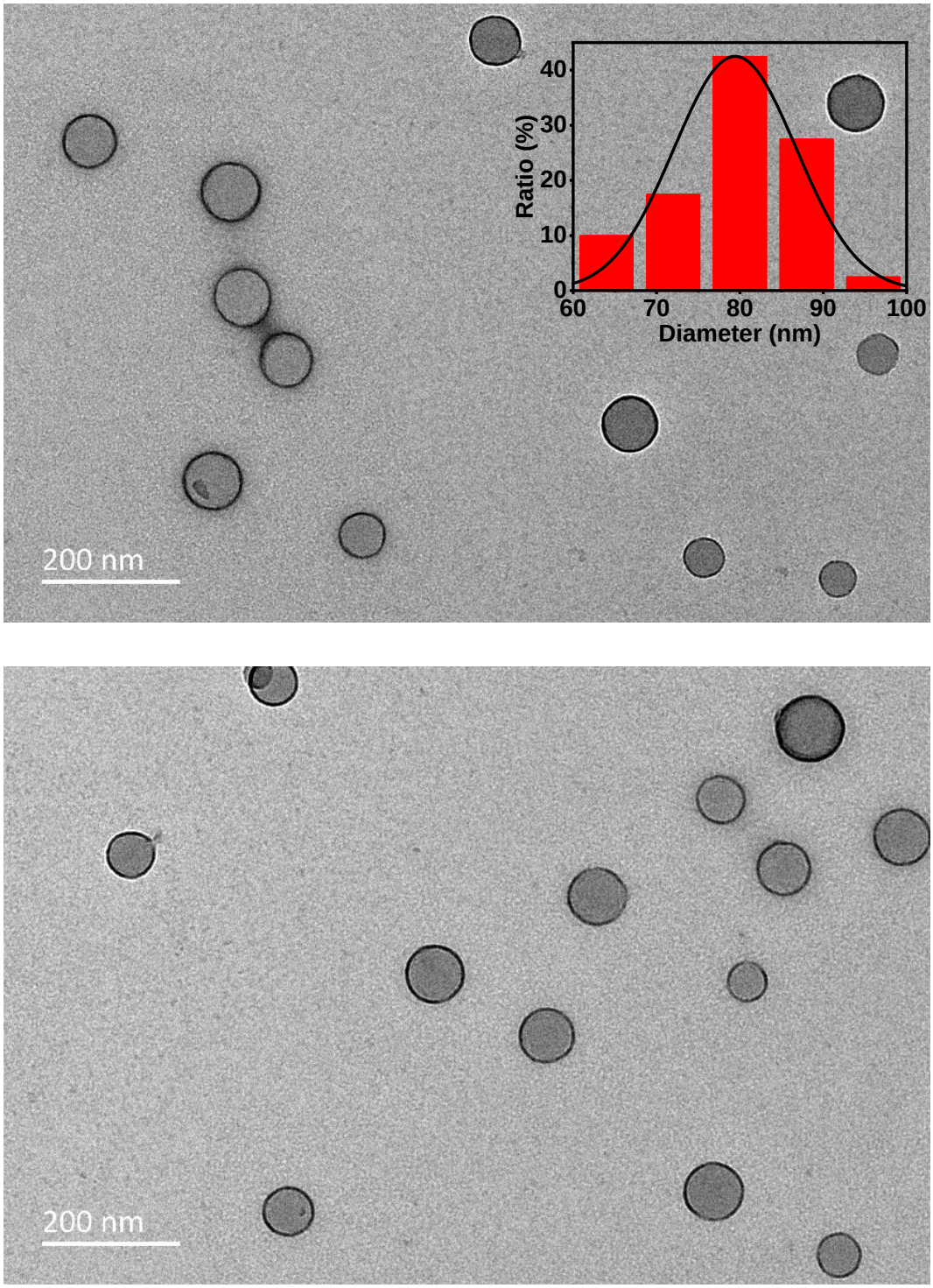

Figure S29. Original HRTEM images showing the self-assembly structures of PBEC$_{12}$A-CP[6] at molar ratio of 16:1. Inset: the histogram analysis of the diameter of vesicles.

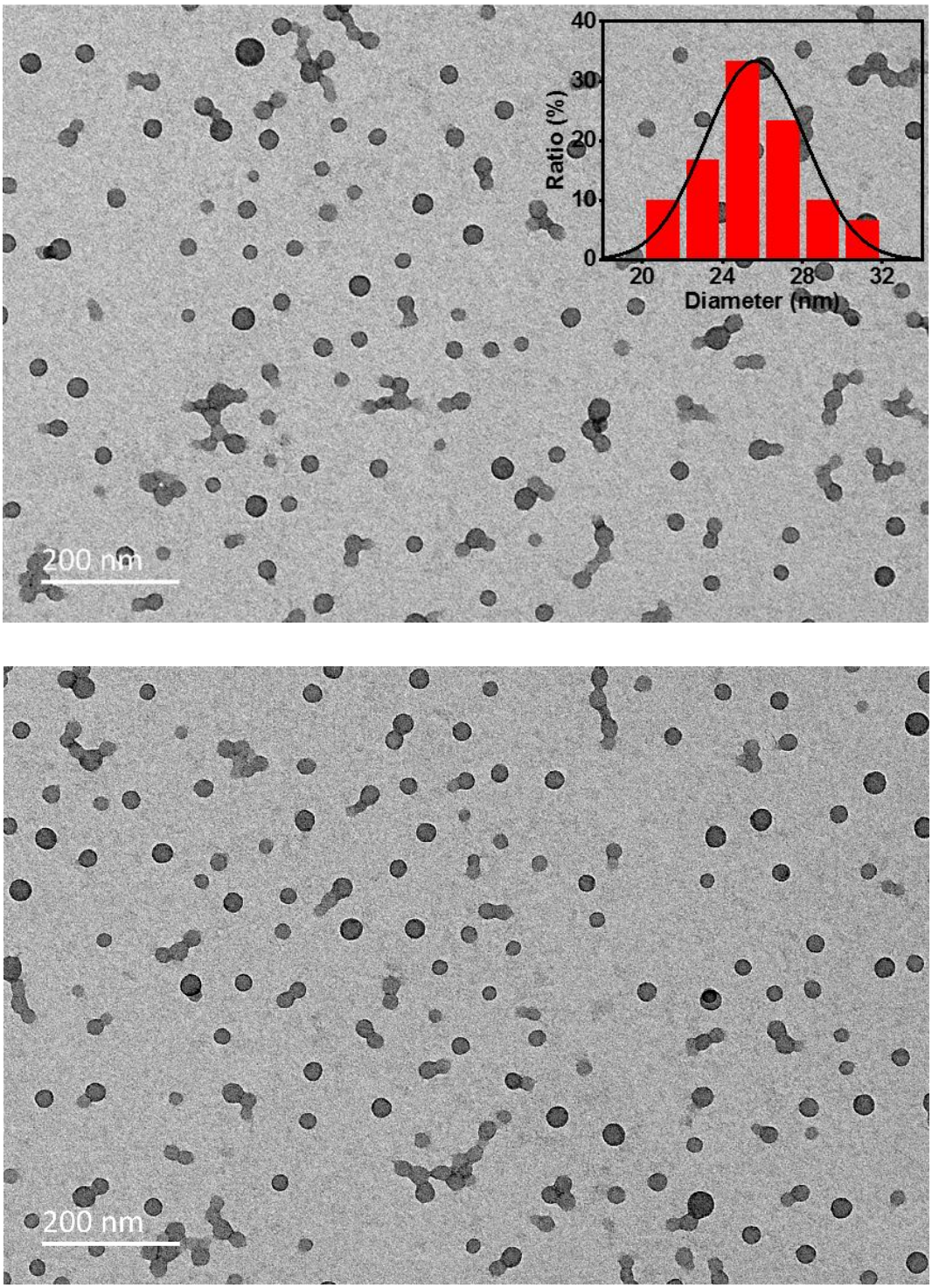

Figure S30. Original HRTEM images showing the self-assembly structures of PBEC$_{12}$A-CP[6] at molar ratio of 12:1. Inset: the histogram analysis of the diameter of vesicles.

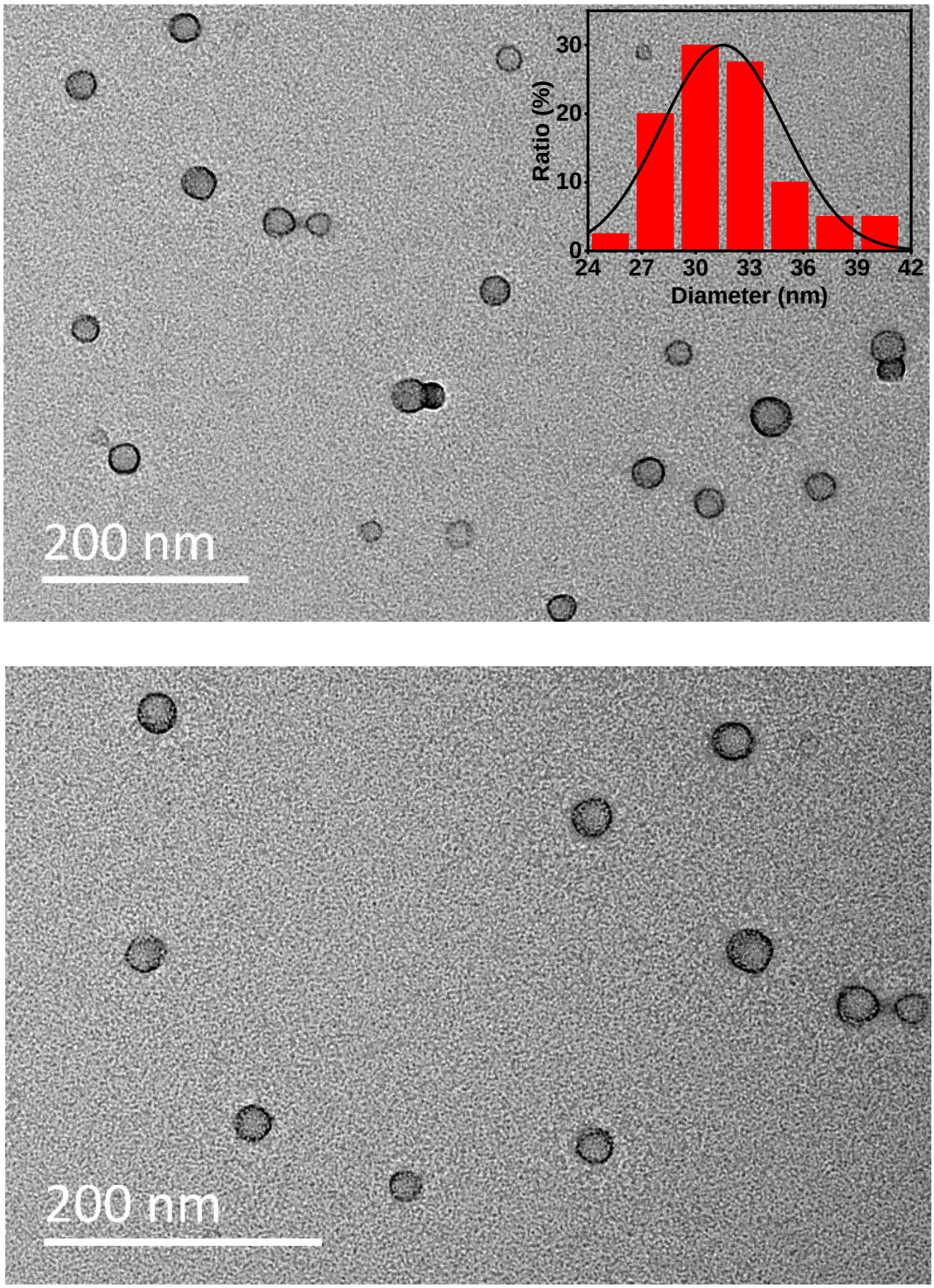

Figure S31. Original HRTEM images showing the self-assembly structures of PBEC$_{12}$A-CP[6] at molar ratio of 10:1. Inset: the histogram analysis of the diameter of vesicles.

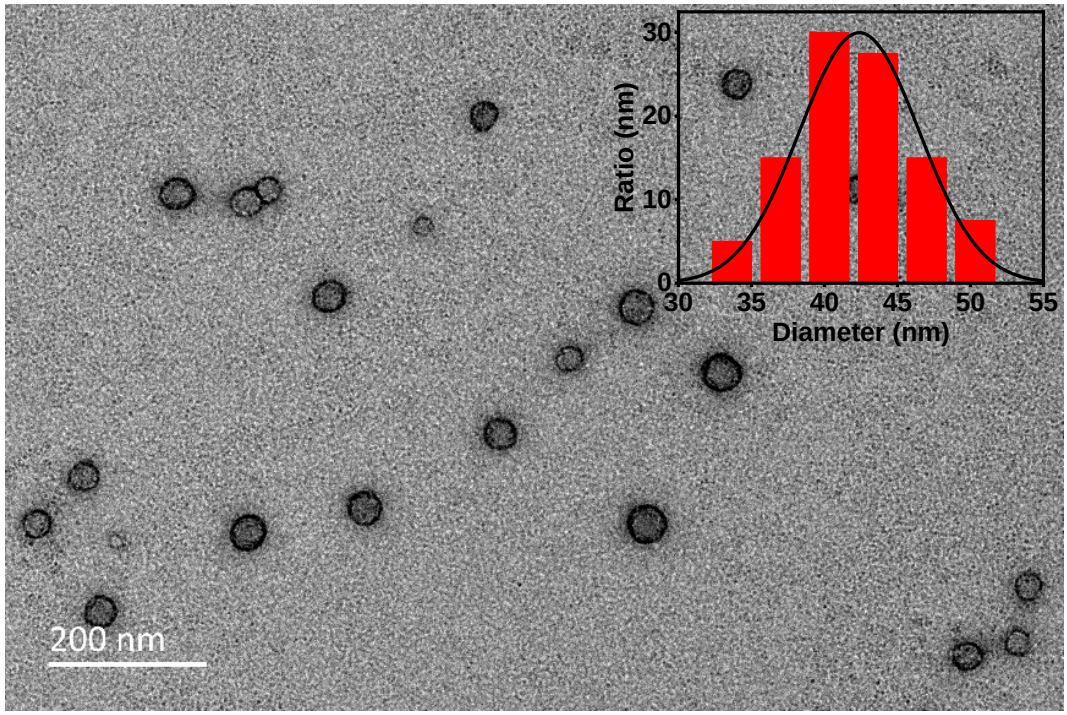

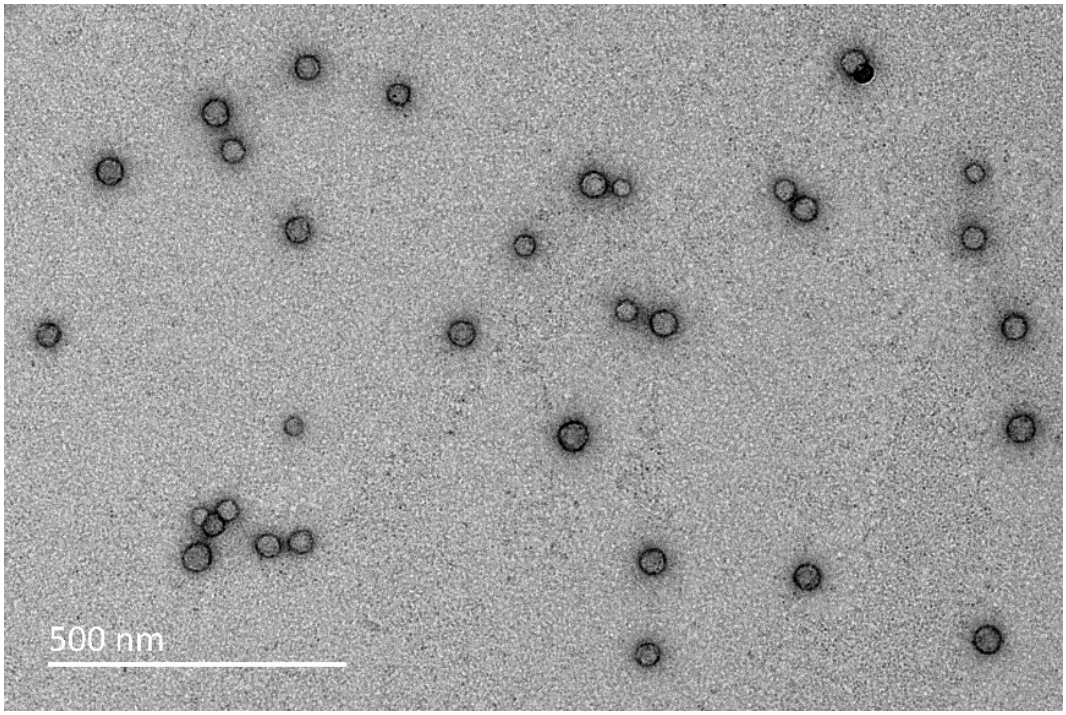

Figure S32. Original HRTEM images showing the self-assembly structures of PBEC$_{12}$A-CP[6] at molar ratio of 5:1. Inset: the histogram analysis of the diameter of vesicles.

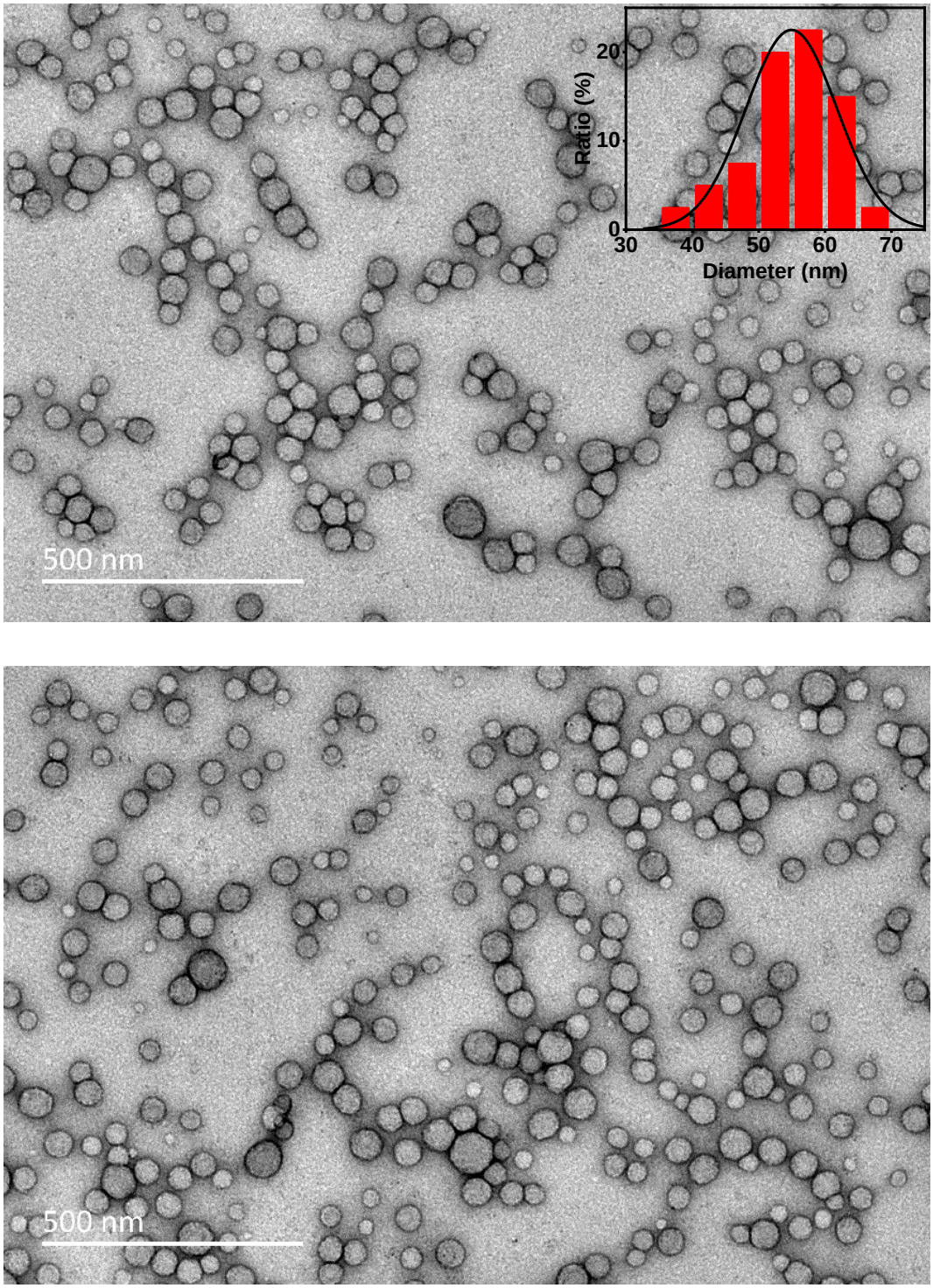

Figure S33. Original HRTEM images showing the self-assembly structures of PBEC$_{12}$A-CP[6] at molar ratio of 4:1. Inset: the histogram analysis of the diameter of vesicles.

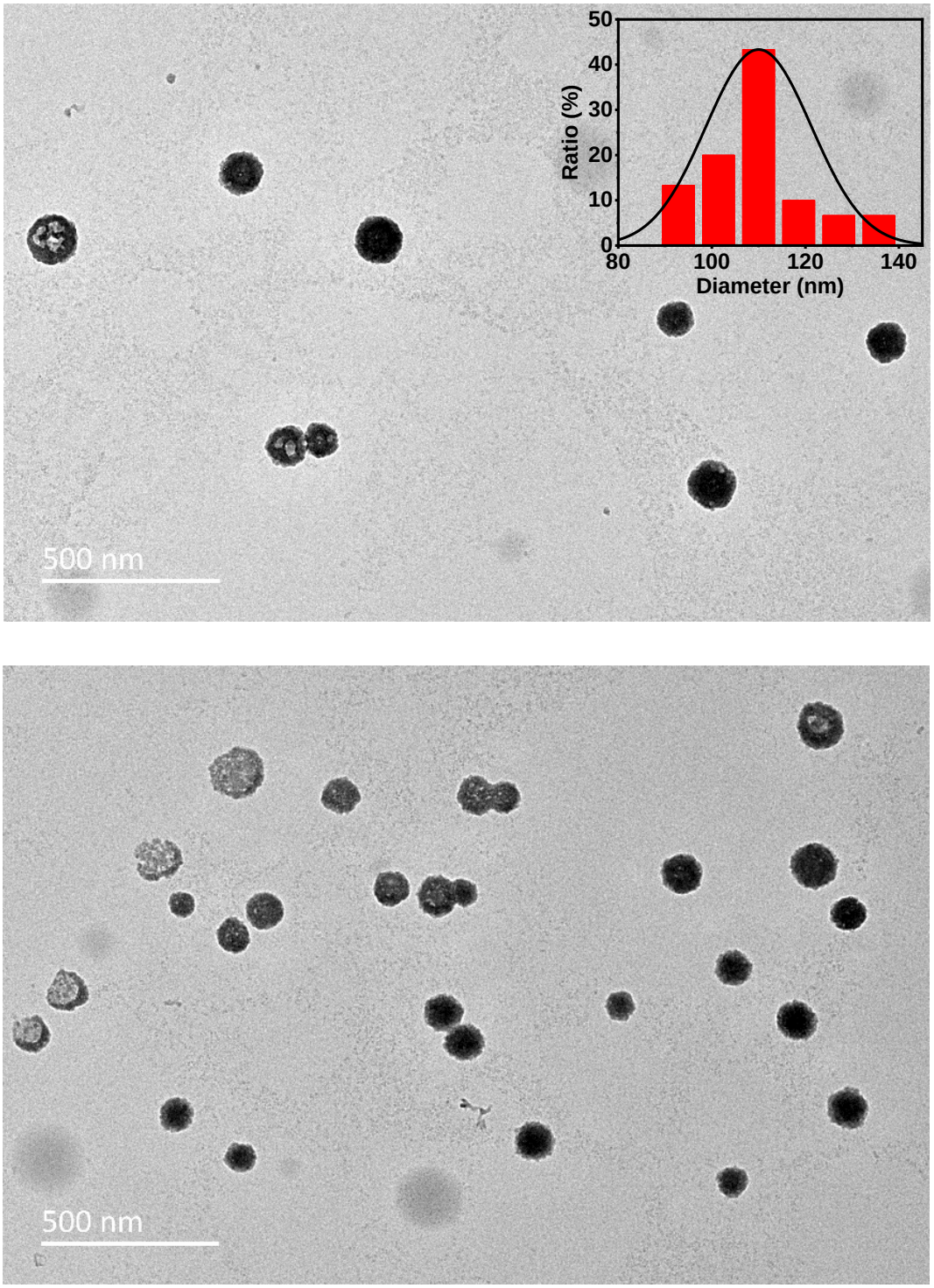

Figure S34. Original HRTEM images showing the self-assembly structures of PBEC$_{12}$A-CP[6] at molar ratio of 2:1. Inset: the histogram analysis of the diameter of vesicles.

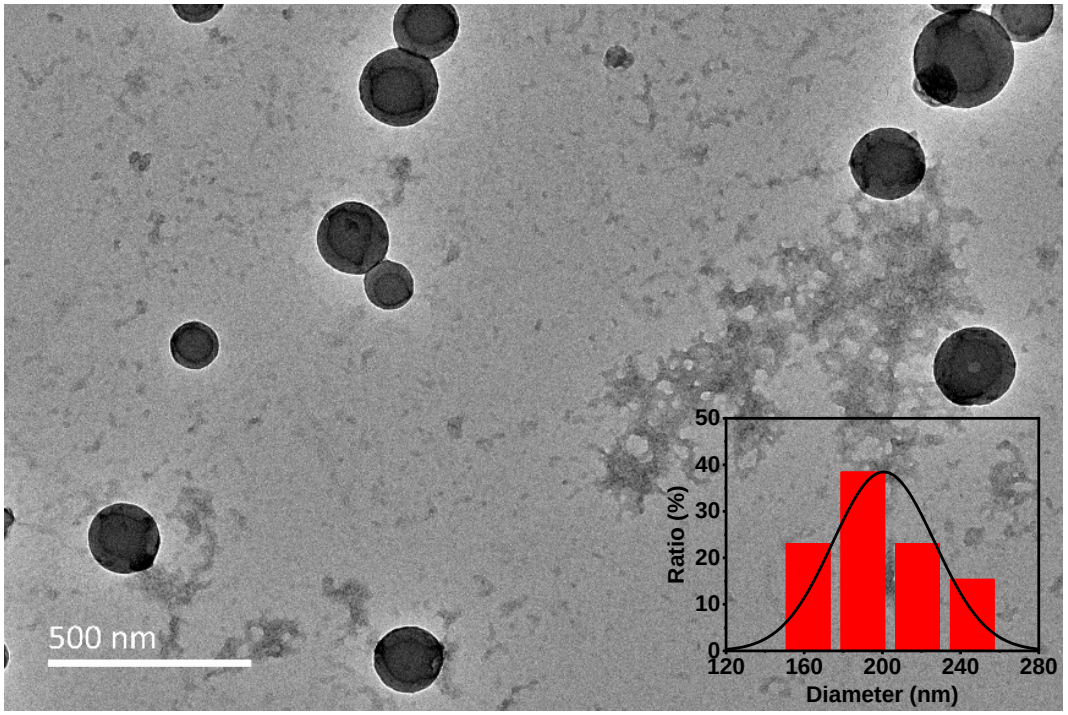

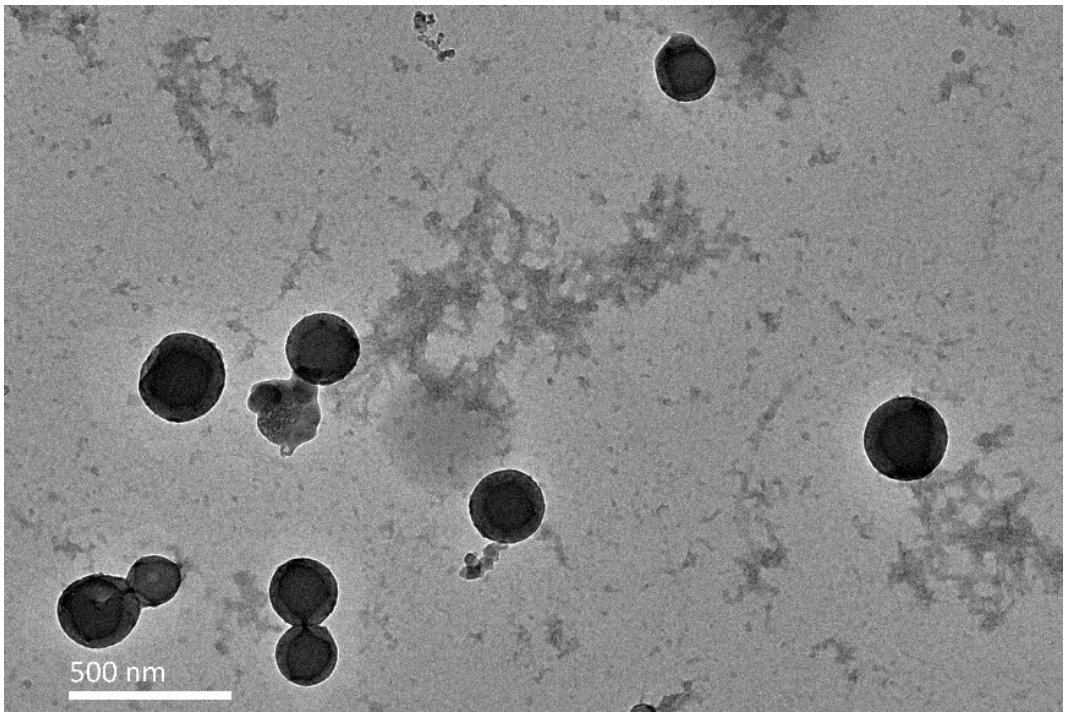

Figure S35. Original HRTEM images showing the self-assembly structures of PBEC$_{12}$A-CP[6] at molar ratio of 4:3. Inset: the histogram analysis of the diameter of vesicles.

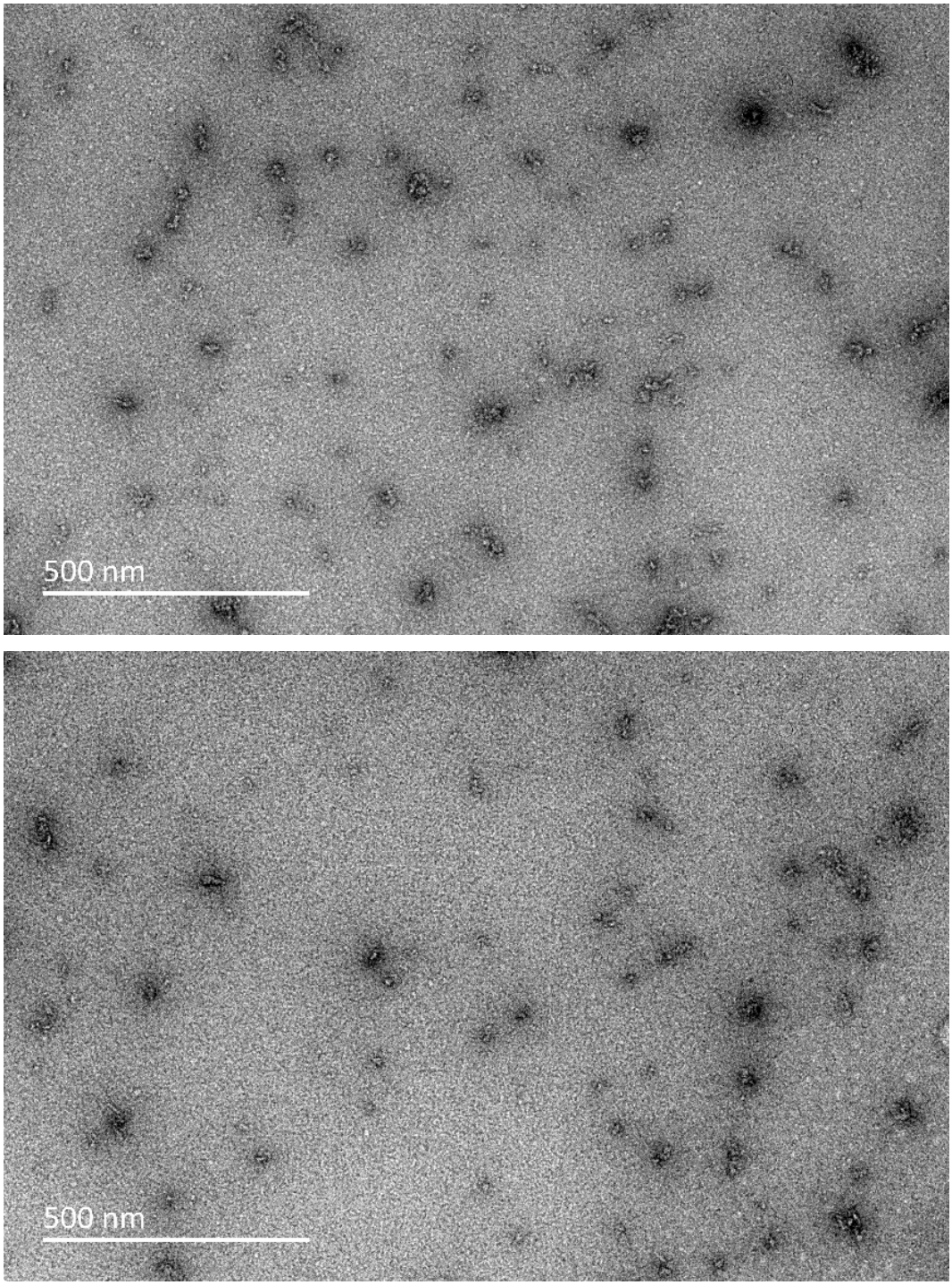

Figure S36. Original HRTEM images showing the self-assembly structures of PBEC$_{12}$A-CP[6] at molar ratio of 1:1.

8. ^{1}H NMR spectra of the host-guest complexation between $C_{12}AH$ and CP[6]

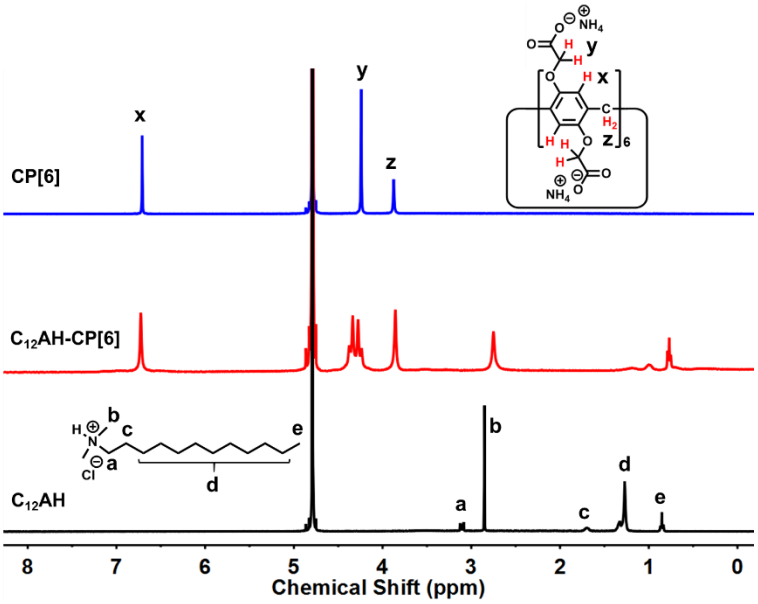

Figure S37. ^{1}H NMR spectra (400 MHz, D_2O) of $C_{12}AH$ (1.0 mM), $C_{12}AH$ in the presence of one equivalent of CP[6] (1.0 mM) and individual CP[6] (1.0 mM) from bottom to top, respectively.

References:

[1] Peng, H. Q.; Liu, B.; Wei, P. F.; Zhang, P. F.; Zhang, H. K.; Zhang, J. F.; Li, K.; Li, Y.; Cheng, Y. H.; Lam, J. W. Y.; Zhang, W. J.; Lee, C. S.; Tang, B. Z. Visualizing the Initial Step of Self-Assembly and the Phase Transition by Stereogenic Amphiphiles with Aggregation-Induced Emission. *ACS Nano* **2019,** *13*, 839-846.